Finite element analysis applied to ergonomic design of 2-piece aluminum beverage cans and bottles

DETC2007-34940

FINITE ELEMENT ANALYSIS APPLIED TO ERGONOMIC DESIGN OF 2-PIECE ALUMINUM BEVERAGE CANS AND BOTTLES

Jing Han
Universal Can Corporation
Sunto-gun, Shizuoka, 410-1392
Japan

Koetsu Yamazaki
Kanazawa University
Kanazawa, Ishikawa, 920-1192
Japan

Sadao Nishiyama
Universal Can Corporation
Tokyo, 112-8525
Japan

Ryoichi Itoh
Universal Can Corporation
Sunto-gun, Shizuoka, 410-1392
Japan

ABSTRACT

This paper has introduced the finite element analysis (FEA) into the ergonomic design to evaluate the human feelings numerically and objectively, and then into the optimization design of beverage containers considering human factors. In the design of the end of can (the lid of can), experiments and the FEA of indenting vertically the fingertip pulp by a probe and the tab of end have been done to observe force responses and to study feelings in the fingertip. A numerical simulation of finger lifting the tab for opening the can has also been performed, and discomfort in the fingertip has been evaluated numerically to present the finger-accessibility of the tab. The comparison of finger-accessibility between two kinds of tab ring shape designs showed that the tab that may have a larger contact area with the finger is better. In the design of beverage bottles served hot drinks, the FEA of tactile sensation of heat has been performed to evaluate numerically the touch feeling of the finger when holding the hot bottle. The numerical simulations of embossing process have also been performed to evaluate the formability of various rib-shape designs. The optimum design has then been done considering the hot touch feeling as well as the metal sheet formability.

INTRODUCTION

Aluminum beverage cans have been developed for more than thirty years, and two-piece aluminum beverage bottles with a screw top have also been launched on to the market recent years to meet new drinking custom of consumers [1-2]. Structure optimization methods based on the finite element analysis have been applied to design optimum shapes and dimensions of aluminum beverage cans and bottles [3-5]. With functional performances such as the sealability and various strength requirements of containers are being satisfied, universal designs based on human factors are expected to increase the comfort level of consumers when drinking from the can or bottle. Survey of consumers or trained panelists is a popular way to evaluate a product ergonomically. Measurement of changes in physiological signals of human subjects, such as blood pressure, muscular load and fatigue and so on, is performed frequently, when using trial products. However, we need some objective, measurable laboratory standards, which can be linked to subjective perceptions of comfort, to predict whether a particular design will be felt comfortable or not by the consumers in the product designing processes.

Figure 1 shows the easy-open can with a SOT (Stay-On-Tab) end. The finger-accessibility is used to evaluate whether it is easy to insert fingertip into the gap between the ring and the finger-deboss of can end, and whether it is discomfort when lifting the ring for opening the can. The easier the finger can be inserted and the ring can be lifted, the better the finger-accessibility is evaluated. To improve the finger-accessibility, various methods have been developed. For example, deepening the finger-deboss, curving up the ring, or applying scores to the panel under the tab so that the tab ring may float up a little
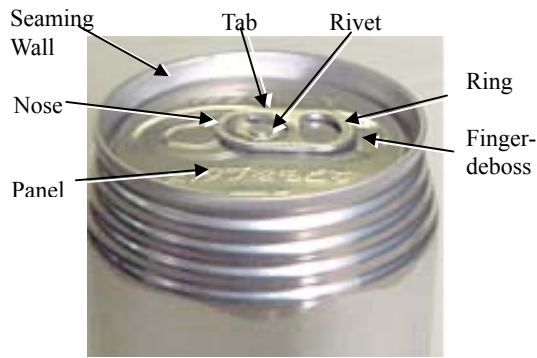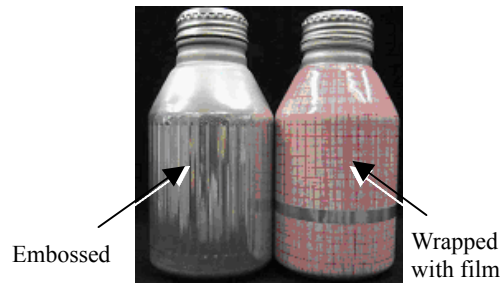
Figure 1. Beverage can.

Figure 2. Beverage bottle.

when the can is filled with beverages and pressured [6]. All of these methods are trying to enlarge the gap between the ring and the finger-deboss to make fingertip go into the gap easily and consequently to improve the finger-accessibility. Since there are limitations of these methods, such as a clearance restriction between the tab and the top edge of the seaming wall, the geometrical shapes of the ring are required to be investigated.

Figure 2 shows the beverage bottle for hot vending. In winter, beverages are expected being offered hot. However, when aluminum bottles are warmed up to about $60^{o}C$ in vending machines, they are too hot to be held by hand due to the high thermal conductivity of aluminum. Therefore, in developing the aluminum beverage bottles for hot vending, it is also necessary to take the tactile sensation of heat into consideration. In order to make aluminum bottles adaptable to hot vending market, two ways are developed. One way is to wrap bottle bodies with a printed PET (PolyEthylene Terephthalate) label to reduce the thermal conductivity, and another one is to add ribs to the bottle wall by an embossing process. The ribs can reduce the amount of heat transmitted to the finger and the air gap between the embossed body and the PET label can weaken further the heat transfer. Influence of the rib dimensions to the touch feeling and embossing formability are required to be investigated.

On the other hand, the fingertip is the most sensitive and important part of human body to obtain information by touching an object and to control manipulation. Studies on sensory receptors in the glabrous skin of the hand, their roles in sensation and their densities within various skin regions can be found in many literatures. The fast-conducting, large-diameter afferent nerve fibers (A-beta-fibers) belong to mechanoreceptive units, whereas the slower-conducting, small-diameter fibers (A-delta-fibers and C-fibers) belong to nociceptive units and thermosensitive units. The mechanoreceptive units are responding to skin deformation during fingertip loading. When only nociceptive units and thermosensitive units are functioning, one can perceive pain and temperature [7-9]. Experiments of presenting stimuli with spherically curved surfaces to the fingertip pulps of human

subjects have been performed, and it is observed that an increase in curvature (with no change in contact force) results in a sharper and higher response profile as well as an increase in perceived contact force [10]. Perception of surface pressure applied to the fingers has been investigated experimentally, and the pressure level at which human subjects perceived a pain was measured as the pain pressure threshold [11-13]. Moreover, the surface shape design method that took the tactile sensation into consideration has been proposed and the surface temperature has been used to present warmness of the surface [14]. Great progress has been achieved in digital human body modeling, but behavioral models with perceptive abilities are still under constructing [15].

Experimental results show that the fingertip is almost incompressible for a point indenter, with the highest change in volume occurring at the largest depth of indentation [16]. The finite element analyses have been performed to predict surface deformations of the fingertip [17], and a geometry and a structural model of the fingertip pulp supported by experimental data have been developed to predict the force-displacement and force-contact area responses of the human fingertip during contact with a flat, rigid surface [18]. However, no works can be found on observing the relation between the pain and the force-displacement curves when a load is applied to the fingertip pulp.

This paper introduces the finite element analysis (FEA) into the ergonomics design to evaluate the human feelings numerically and objectively, and then into the optimum design of beverage containers considering human factors. Two ergonomics design examples of the beverage containers based on numerical evaluations of human feelings are shown. In the ergonomics design of the end, experiments of indenting vertically the fingertip pulp by a probe and the tab of end are carried out to observe force responses and to study feelings in the fingertip. The FEA is performed to simulate the tab indenting the fingertip vertically for developing the finite element model of the fingertip. Moreover, a numerical simulation of finger lifting the tab is also performed, and discomfort in the fingertip is evaluated numerically to present the finger-accessibility of the tab. Finally, the comparison of finger-accessibility between two kinds of ring shape designs is made. In the optimum design of beverage bottles for hot vending considering human factors, the FEA of tactile sensation of heat is performed to evaluate numerically the touch feeling in the finger when holding the hot bottle. The numerical analysis includes the contact deformation analysis

2

and heat transfer analysis between the finger and the hot bottle body. The touch feeling of the cylindrical bottle and several embossed bottles with different rib-shape designs are evaluated and compared with each other. The numerical simulations of embossing process are also performed to evaluate the formability of various rib-shape designs. Finally, the optimization design is carried out considering the hot touch feeling as well as the metal sheet formability.

ERGONOMIC DESIGN OF THE CAN END
Experiments on Indenting Human Finger Pulp by a Probe

A tension-compression tester is used for the experiments on indenting finger pulp so that dynamic real-time measurements to track the finger pulp thickness changes and force changes over a very short period may be possible. As shown in Fig. 3(a), the index finger is laid on the table of the tester and then an indenter of probe or tab is moved down at a constant velocity v to indent the finger pulp at the center in width direction and at a distance L from the tip edge of the finger in longitudinal direction. A computer records automatically the force applied to the finger and the displacement of the indenter at every 0.05 second. To avoid any injury to the subjects, an upper limit of the force P_{max} or an upper limit of the displacement H_{max} of the indenter is set in advance. When the force reaches the upper limit P_{max} or the displacement reaches H_{max}, the indenter has been kept stopping for 60 seconds and then been unloaded to its initial position. An aluminum probe with a hemispherical tip 3.68 mm in diameter (Fig. 3(b)) is used to indent vertically the index fingertip pulp of four human subjects (mean age 38yr, age range 28-56yr).

In order to determine the deforming property of finger pulp and to experience the feeling of pain, experiments of the finger pulp indentation at $L = 8$ mm by the probe have been performed. Figure 4 shows the force changes with time and the displacement of the probe at velocities of $v = 4$ mm/min. The force-time relation plotted in Fig. 4(a) shows that when keeping the indented depth of probe after it reaches the upper limit H_{max}, the force decreases with time going by. It is so called stress relaxation due to the viscoelastic property of human finger materials. A typical force-displacement curve, as shown in Fig.4(b), may be simplified as a combination of Part 1, Part 2 and Part 3 as illustrated in Fig.4(c). The upper transverse axis

represents the fingertip thickness T_f that is calculated as $T_f = T_0 - H$, where T_0 is the initial thickness of the fingertip at the center and H is the indentation depth, i.e., the displacement of the indenter. It is observed that the finger thickness decreases almost linearly at Part 1. The thickness decrease rate becomes lower at Part 2, and the thickness decreases almost linearly again but the decrease rate becomes further lower at Part 3. It is considered that when the deformation of soft tissue comes near to its limit, the force required to deform the soft tissue becomes higher and higher.

Concerning the influence of the personal differences in the finger and the indenting velocity of the probe, experimental results of HS1 (Human Subject 1, in 30s, Female), HS2 (30s, Male) and HS3 (50s, Male) are compared in Fig.5, when $v = 1$ mm/min, 4 mm/min. Comparison result shows that the gradient of Part 3 in the force-displacement plot doesn't change much even though the finger dimensions are different person by person. The experimental results agree with those in literatures [19]. Figure 5 also shows the slower the velocity is, the later Part 2 rises. It's because that if the velocity is lower, the indenting time becomes longer, hence, the resistance in the fingertip becomes smaller due to the stress relaxation in the soft tissue. However, the gradient of Part 3 doesn't show a meaningful change in the force-displacement plot.

All human subjects have been asked to report the feeling in fingertips during the indenting. The common feeling change is as follows; we feel a touch at Part 1 of the force-displacement curve, then feel a pressure and our pulse at Part 2, finally feel discomfort followed by a pain in the fingertip at Part 3. The sensation change is because that, with the load increasing, the A-beta-fibers (the sense of touch-pressure), A-delta-fibers (fast pain) and C-fibers (slow pain) in the skin are engaged and the afferent information is conducted to the central nervous systems in sequence. The discomfort and pain in the finger increases as the force or the indentation depth increases. If the total load is the same, the narrower the contact area is, the deeper the indentation depth becomes, i.e. the thinner the fingertip becomes, hence, the greater the discomfort is felt. The perception of pressure applied to the fingertip agrees with earlier investigation results [10-13].

In the numerical analysis of finger access of the tab described later, Part 3 in the feeling diagram is necessary to be
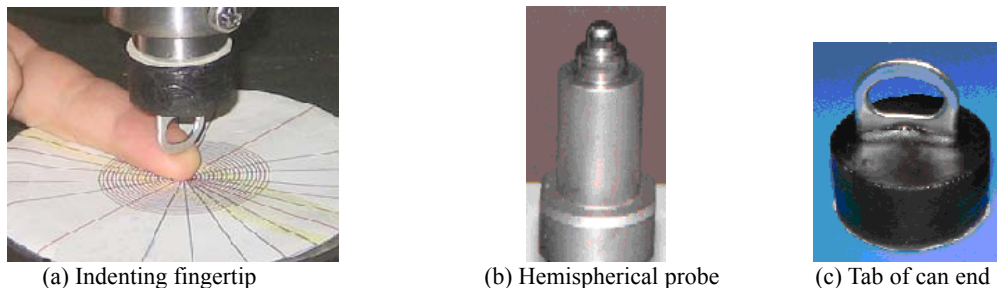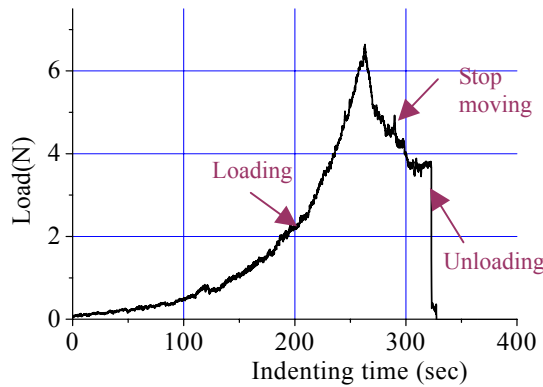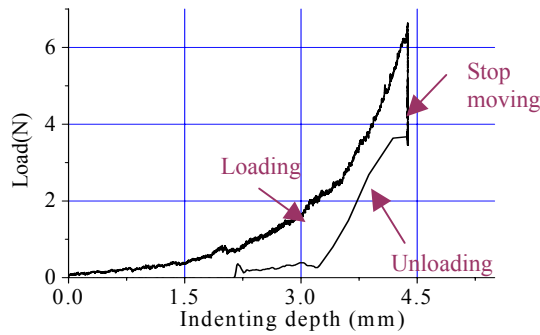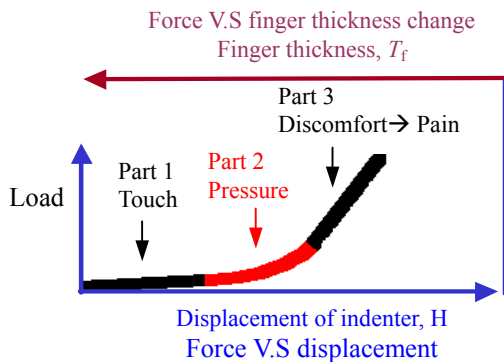

(a) Indenting fingertip　　　　(b) Hemispherical probe　　　(c) Tab of can end
Figure 3. Experimental setup of indenting fingertip.

　　　　　　　　Copyright © 2007 by ASME

(a) Relation between indenting time and load.

(b) Relation between indenting depth and load.

(c) Diagram of feelings in fingertip

Figure 4. Experimental observations of indenting fingertip.

taken into account because we focus on only the feeling of discomfort and pain in the fingertip when lifting the tab to open the beverage can. Therefore, it is judged that the fingertip model can be simplified as an elastic model of a constant value of Young's modulus at Part 3.

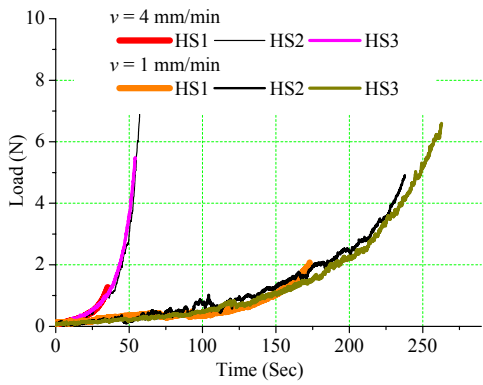## Experiments and FEA of the tab indenting the fingertip

In order to confirm the effectiveness of the finite element model of the fingertip for the numerical analyses of finger-accessibility, the experiments and the numerical simulations of the tab indenting vertically the finger pulp have been performed and compared. The regular tab with the round ring is used as the indenter (Fig. 3(c)). The tab is fixed in a cylindrical resin so that it can be fixed to the tester to indent vertically the index fingertip pulp of human subjects. Since the space under the ring is narrow, the finger cannot be inserted much. Figure 6 shows a typical force-displacement curve obtained in experiments on the tab indenting vertically the finger pulp at L = 2 mm, v = 2 mm/min.

Figure 7(a) shows the schematic diagram of the distal part of fingertip [20]. The fingertip is simplified as an elastic model which consists of two kinds of mechanical properties, the bone and the soft tissue. Figure 7(b) and (c) show the vertical cross-section, transverse cross-section and the whole three-dimensional finite element model of the finger. The mechanical properties of bone and soft tissue of fingertip model are assumed as: Young's modulus E_1 = 17 GPa, E_2 = 5 MPa, and Poisson's ratio v_1 = 0.3, v_2 =0.45, respectively [21]. The model is descritized into eight-node solid elements. Figure 8 shows the analysis model. The tab ring is assumed as a rigid body in the finger indenting simulation, where the finite element code, MSC.MARC is utilized.

The experimental results and the numerical analysis results are compared in Fig. 6. The upper transverse axis indicates the indenting depth obtained by numerical analysis, and the lower transverse axis indicates the indenting depth measured in the experiment. Comparing the analysis results to the experimental results, it is clear that the rear part of the force-displacement curves agrees very well with each other. Therefore, it can be concluded that the finite element model of the finger is available for the finger-accessibility analysis to evaluate numerically discomfort and pain in the fingertip.

Numerical Analysis of the Finger-accessibility

Figure 9 shows the standard opening action of the beverage can with SOT end [22]. There are four steps, the first step is to lift up the ring by the index finger while pressing the tab nose by the thumb, the second step is to lift up the tab completely forward and the third step is to push the tab back down. It is ready for drinking when the tab stays on the can as shown in the last step. In the first step, pressing the tab nose by the thumb can make the ring rise up a little naturally and can prevent the ring slipping down along the surface of the index finger pulp so that the finger can be easily inserted into the space under the ring. Although there are many ways to open the beverage cans by consumers, the common points are the fingertip and the ring. To evaluate the touch feeling of discomfort or pain in the finger when lifting up the ring, the

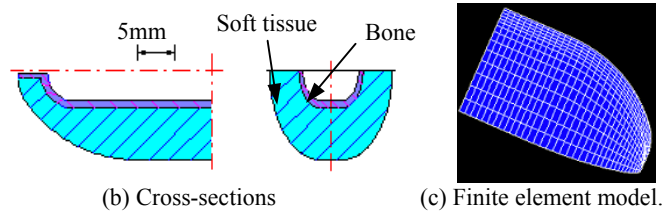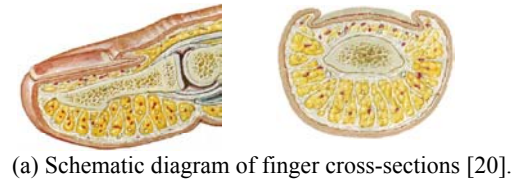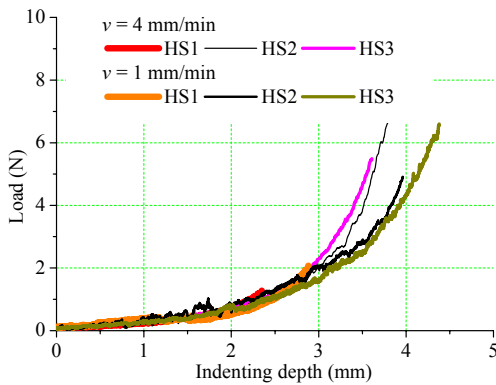(a) Relation between indenting time and load.

(b) Relation between indenting depth and load.
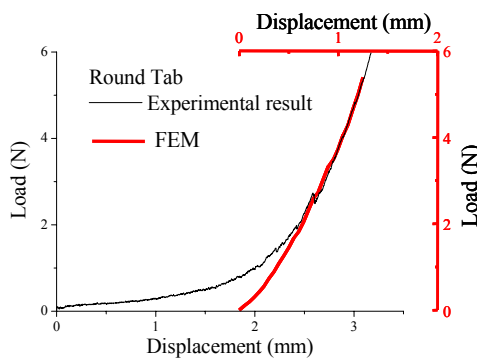**Figure 5. Observations of personal differences.**

Figure 6. Comparison between simulation results and experimental ones.

finger-accessibility analysis model is developed as shown in Fig. 10. Assuming the deformations of tabs and the finger models are symmetry to the central vertical plane, the numerical analyses on 1/2 finite element model is performed.
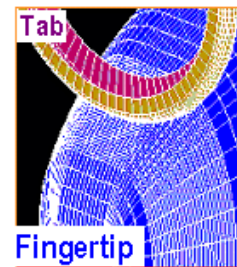

(a) Schematic diagram of finger cross-sections [20].

(b) Cross-sections   (c) Finite element model.
Figure 7. Model of distal part of human finger.

Figure 8. Analysis model of indenting finger by a tab

All freedoms of the nodes on the circular edge of the rivet part of the tab are fixed. The edge nodes of the bone elements on the tip of the finger model are enforced to move 0.5 mm forward and then move upper forward to simulate the process of fingertip lifting up the tab. The maximum value of the contact normal stress of the finger model when lifting up the tab is used to represent the perception in the finger. The smaller the contact stress is, the less discomfort the finger experiences and the better the finger-accessibility of the tab is evaluated.

The material model used for the aluminum tab is assumed as an elasto-plastic von Mises material with isotropic hardening. The Young's modulus $E_3 = 70$ GPa, Poisson's ratio $v_3 = 0.33$ and yielding stress $\sigma = 260$ MPa are assumed. The tab model is descritized into four-node shell elements with 0.33 mm thickness.

In order to investigate the effect of geometric shape of the ring, the round ring (Model 1) and the concave ring (Model 2), are modeled as shown in Fig.11. Model 2 is designed to fit the shape of finger pulp. The length of the symmetric central lines and the symmetric central cross-sections of two tab models are the same.

Figure 12 shows the deformation of the fingertip pulp and Fig. 13 shows the contact normal stress distribution of finger model when the tab models are lifted 2.5 mm. It is obvious that
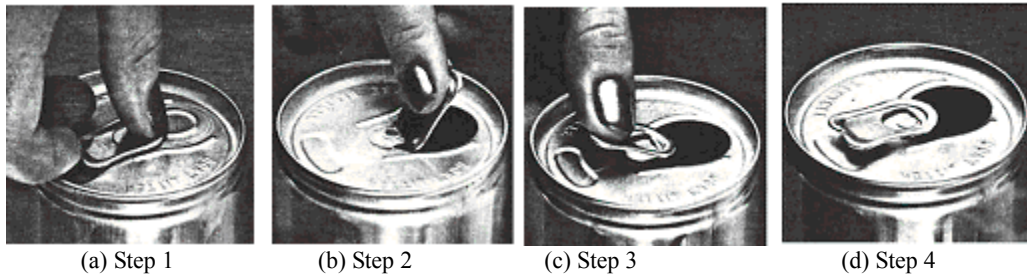
(a) Step 1   (b) Step 2   (c) Step 3   (d) Step 4
Figure 9 Procedures for opening SOT ends [22].
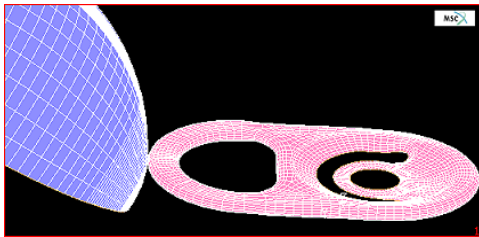
Figure 10. Analysis model of finger-accessibility.
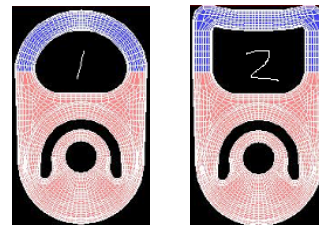
(a) Model 1   (b) Model 2
Figure 11. Finite element models of tabs.
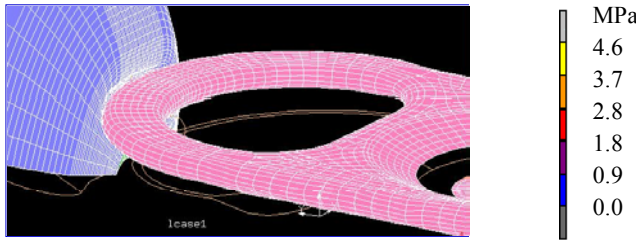
Figure 12. Simulation result of lifting up tab.

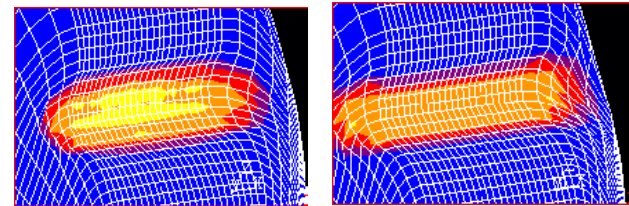(a) Model 1   (b) Model 2
Figure 13. Simulation result of lifting up tab.

the stress concentration occurred at the part in contact with the central part of the round ring. When the displacement of the ring center (H_1) becomes 2.5 mm, the finger can be inserted more and the ring can be re-held for an easy open. The difficulty is evaluated by the can openability rather than the finger-accessibility when H_1 is larger than 2.5 mm, so the simulation results before H_1 becomes 2.5 mm are observed. The maximum value of the contact normal stress, the contact areas, and the maximum value of the equivalent elastic strain of the finger are compared in Fig.14. In the case of the tab with a concave ring, the contact area between the finger and the ring is larger and the maximum value of the contact normal stress and equivalent strain are smaller. It is considered that if a larger area shares the load that required for lifting up the tab, the contact normal stress and equivalent strain may become lower; hence discomfort in the finger may decrease more. Therefore, it is concluded that the finger-accessibility of the tab that may have a larger
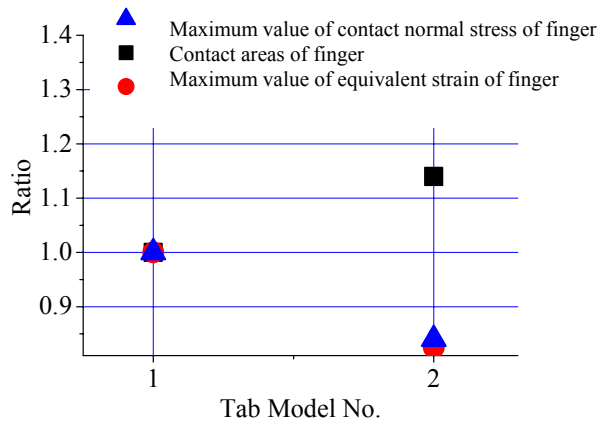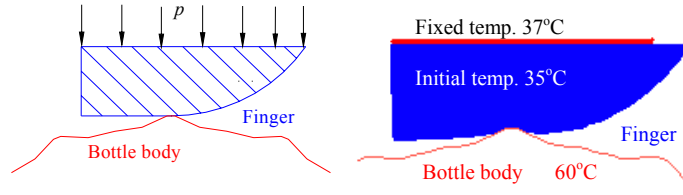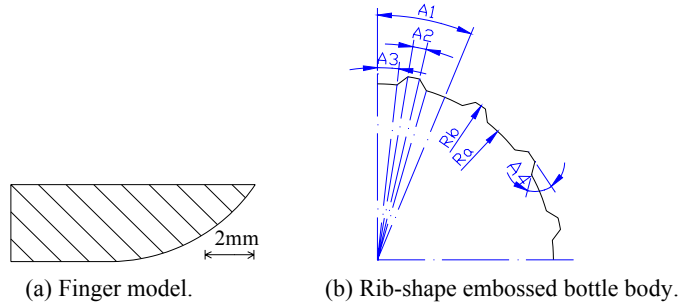

Figure 14. Contact normal stress distributions of finger models.

(a) Finger & bottle   (b) Contact analysis model   (c) Heat transfer analysis model

Figure 15. Analysis model of tactile sensation of heat.

(a) Finger model.   (b) Rib-shape embossed bottle body.

Figure 16. Cross-sections.

TABLE 1. Dimensions of embossed body models.

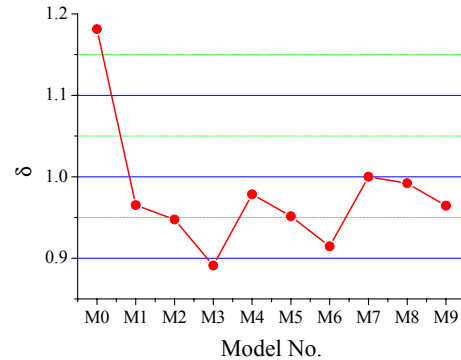| Model	A_2 (Degree)	A_3 (Degree)	A_4 (Degree)
M0	--	--	--
M1	1.5	1.5	17.89
M2	1.5	3.5	20.35
M3	1.5	5.5	25.26
M4	3.5	1.5	19.92
M5	3.5	3.5	23.36
M6	3.5	5.5	30.57
M7	5.5	1.5	22.35
M8	5.5	3.5	27.26
M9	5.5	5.5	38.23

Figure 17. Heat transfer analysis results.

contact area with finger is better. The finger-accessibility of the tab with a concave ring is better than that of the tab with a round ring.

ERGONOMICS DESIGN OF THE BOTTLE BODY
FEA of the Tactile Sensation of Heat

In order to evaluate numerically the touch feeling of the finger when holding the hot beverage bottle, the finite element analyses of the tactile sensation of heat are performed. Numerical analyses of the tactile sensation of heat include contact deformation analyses and heat transfer analyses between the finger and the rib-shape embossed bottle body, as shown in Fig.15. In the contact analyses, the fingertip is contacted with the mountain of rib, and a distributed load p toward the bottle is applied to the upper surface of the finger model. The deformed configuration of finger obtained in the contact analysis is then used in the heat transfer analyses. Figure 16 shows the cross sections of the fingertip and rib-shape embossed bottle body. The complex inside detail of the finger structure is neglected and the cross section of the finger model is simplified by taking 25 mm from the fingertip and 8 mm from the contact point. The embossed body of sixteen ribs is considered in this paper, i.e., $A_1 = 22.5^\circ$. The values of radii used for the analysis of the tactile sensation of heat are $R_a = 32$ mm, $R_b = 33.15$ mm. The finger model is descritized into four-

node quadrilateral elements, and the embossed bottle is assumed as a rigid body of 60°C. The initial temperature of the finger is set as 35°C and the temperature of the nodes on the upper surface of the finger model are fixed as 37°C. Experiments have been done to measure the temperature changing on the fingertip surface when grasping the hot bottle, and the numerical simulations have been performed using several different values of the contact heat transfer coefficient to fit the experimental observations. The finite element code, MSC.MARC, is used to simulate the configuration change of the finger and to calculate the amount of heat transmitted from the hot bottle to the flesh of the finger when grasping the embossed bottle body.

In order to gain a deeper understanding of the influence of rib dimensions A_2, A_3 and A_4 to the tactile sensation of heat, model M0 with no embossing process and nine embossed body models listed in Table 1 are analyzed. It is clear that with the angle A_2 or A_3 increasing, A_4 increases and the slope of the mountain and valley of the rib becomes steeper.

The amount of heat transmitted from the bottle in a unit time is calculated using Eq.(1),

$$Q = c \cdot \sum_{i=1}^{n} S_i \cdot (\overline{T}_i - \overline{T}_{i0}) \quad , \tag{1}$$

where, n is the number of elements, S_i is the area of the element i, $\overline{T}_{i0}$ and $\overline{T}_i$ are the initial mean temperature and the mean temperature at a unit time of element i, respectively. The ratio of the amount of heat transmitted from the hot bottle is calculated as $\delta = Q/Q_0$, where Q_0 is the amount of heat transmitted from the bottle model M7 when $p = 2.5$ MPa is applied to the finger model.

The heat transfer analysis results at 0.03 second are compared in Fig.17 for all models. It is obvious that all embossed bottle body models transfer less heat to the finger than the un-embossed cylindrical body model M0 does. Figure 18 shows the temperature distribution of the finger model at 0.03 second when grasping hot bottle models. It is found that the temperature of the finger grasping embossed bottle body is lower than that of un-embossed bottle body. From the comparison of the amount of heat transmitted from the hot

bottle body, it is clear that the sharper the mountain of the rib is, the smaller the contact area becomes and then the less the heat is transmitted. It is concluded that the rib-shape of the embossed bottle of relatively small value of A_2 as well as large value of A_4 has better touch feeling.

Simulations of Rib-Shape Embossing Process

The axial embossing method is to emboss the bottle by imposing axially a cylindrical tube die with the rib-shaped inner surface on the outer surface of the bottles. For manufacturability purpose, the necking, screw forming and embossing processes can be finished by only one horizontal-axis rotary machine, however, the quality is dependent on the shape of ribs and the forming condition.

Figure 19(a) shows the analysis model of the axial embossing process. Nonlinear finite element code, MSC.MARC, is used to simulate the cylindrical tube die with the rib-shaped inner surface imposing axially on the outer surface of the bottle body. The dimensions of the bottle body and die are illustrated in Fig. 19(b) and (c), respectively. The length of the die model is 35 mm. Since the bottle body is axisymmetric, a 1/4 model is descritized into 4-node quadrilateral shell elements. The sidewall thickness of the bottle body is 0.13 mm. The die is treated as a rigid body with $R_c = 32$ mm and $R_d = 33.15$ mm. The number of ribs is specified as 16, i.e., $A_1 = 22.5°$.
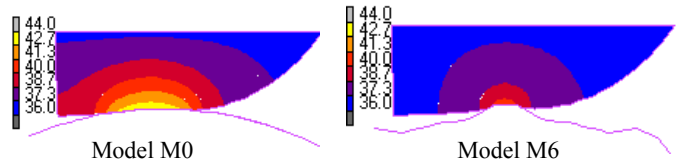

Model M0   Model M6

Figure 18. Temperature distribution of the finger model.

(a) Axial embossing model   (b) Bottle body model (unit: mm)   (c) Cross-section of die
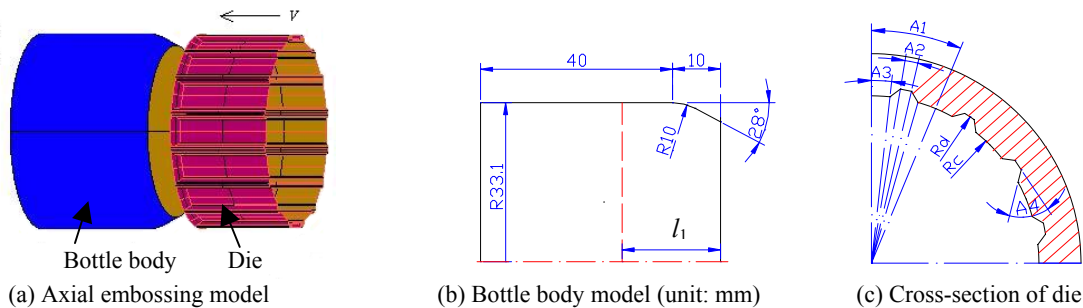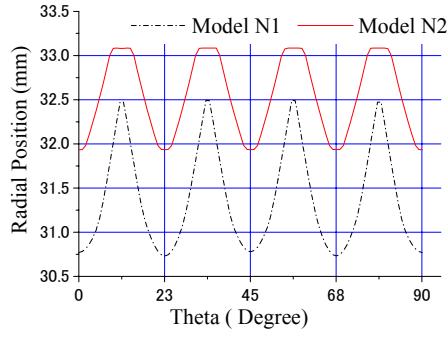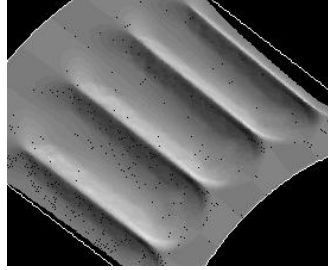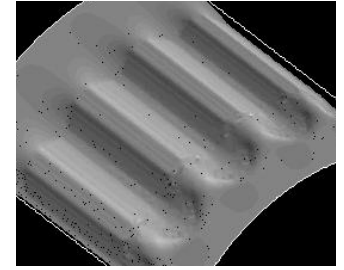
Figure 19. Simulation model of embossing process.

(a) Radial position　　　　　　　(b) Deformation of model N1　　　　　　(b) Deformation of model N2

Figure 20. Simulation results of the embossing process.

The embossing process simulations are performed using two die models, model N1 ($A_2 = 1.5^\circ$, $A_3 = 5.5^\circ$) and N2 ($A_2 = 5.5^\circ$, $A_3 = 1.5^\circ$). Figure 20 shows the radial positions of nodes at a section with an original axial distance $l_1 = 20.5$ mm from the shoulder side, and shows the embossed bottle body models. It is observed the embossed bottle body dented much when using the dies like model N1 with a relatively large value of A_3. And the smaller the value of A_2 is, the more the embossed body dented and the worse the embossing formability becomes.

The mean radii of the mountain and valley of the rib-shape embossed bottle body, R_1 and R_2, are used to evaluate the axial embossing formability. R_1 and R_2 of the embossed body are smaller than R_d and R_c of the die, respectively. For example, for model N2, $R_1 = 33.09$ mm, $R_2 = 31.94$ mm and then $\Delta R = R_1 - R_2 = 1.15$ mm.

Optimum Design of Bottle Body

On the basis of the numerical analyses of the tactile sensation of heat and the axial embossing process simulations, the hot touch feeling and embossing formability of bottle with ribs can be evaluated numerically. Since the dimensions of ribs influence the touch feeling as well as the embossing formability, it is necessary to perform a multi-objective optimization subject to the rib dimension constraints. The Response Surface Approximation (RSA) method and the Weighted Sum approach of the multi-objective optimization techniques are applied to optimize the embossed bottle considering both of the touch feeling and the embossing formability [23]. The problem is posed as:

Design variables: $X = \{x_i\}$, $i = 1,...,n$

(n : the number of design variables)

Minimize: $f = w_1 \cdot f_1 + w_2 \cdot f_2$　　　　　(2)

$$f_1 = \frac{Q(X)}{Q_0},$$　　　　　(3)

$$f_2 = \frac{\Delta R_0}{R_1(X) - R_2(X)},$$　　　　　(4)

subject to: $g_1 = 1 - R_1(X)/R_{1\min} \leq 0$,　　　　　(5)

$g_2 = 1 - R_2(X)/R_{2\min} \leq 0$,　　　　　(6)

$x_i^L \leq x_i \leq x_i^U$, $i = 1,...,n$　　　　　(7)

where, f_1 is for evaluating the hot touch feeling and f_2 is for evaluating the embossing formability. The weight coefficients w_1 and w_2 are defined as $w_1 + w_2 = 1$, $0 \leq w_1, w_2 \leq 1$. $R_{1\min}$ and $R_{2\min}$ are the allowable minimum values of the mean radii (R_1, R_2) of the mountain and valley of the rib-shape embossed bottle body; Q_0 and ΔR_0 are scalars. x_i^U and x_i^L are the upper and lower bounds on design variable i, respectively.

At first, the design variables and levels are defined and the design points are assigned by an orthogonal array in the design-of-experiment technique. The numerical analyses of the tactile sensation of heat and embossing process simulations are then carried out for all design points. On the basis of the numerical results, approximate functions of the amount of heat (Q), the mean radii (R_1, R_2) of mountains and valleys of the embossed bottle are constructed by the orthogonal polynomials in terms of the design variables. Optimum solution is then calculated. This optimization process is repeated until the given convergence condition is satisfied.

As a numerical example, dimensions A_2 and A_3 of the rib are selected as design variables with three levels of the same interval. The orthogonal array L_9 is used to assign the design points. The lower bounds are 1.5° for two design variables, and the upper bounds are 5.5°, 3.5°, respectively. The constraints are given as $R_{1\min} = 33.05$ mm, $R_{2\min} = 31.91$ mm. According to the embossing condition, designers may decide the weight coefficients, w_1 and w_2. For example, if give $w_1 = 0.4$, $w_2 = 0.6$, the optimum values for A_2 and A_3 are obtained as $A_2 = 3.2^\circ$, $A_3 = 2.5^\circ$, the embossing simulation result is shown in Fig.21, and the amount of heat transmitted from the optimized bottle model decreased at least 30% as compared with that of the regular bottle.

9　　　　　　　　　　　Copyright © 2007 by ASME

CONCLUSIONS

This paper has tried to apply the FEA to evaluate the human feelings numerically in the design of beverage containers. In the design of the can end, the feeling of discomfort and pain when lifting up the tab for opening the can is evaluated numerically. The comparison of two kinds of tab ring shape designs has shown that the tab that may have a larger contact area with the finger is better. In the optimization design of beverage bottles for hot vending, the touch feeling in the finger when holding the hot bottle is evaluated numerically. The bottle body is optimized to have better touch feeling and good metal sheet formability as expected by designers.

The method proposed to evaluate numerically the feelings of the consumer can be applied to design not only the beverage container but also other product that has an interface with human, to make it more comfortable for the consumer.

Figure 21. An optimum model when w_1=0.4 and w_2=0.6.

REFERENCES

[1] Nishiyama, S., 2001, "Development and Future Subjects of Aluminum Beverage Cans," Packpia, **2**, pp.10-15. (in Japanese)

[2] Ueno, H., 2003, "Drinks Cans with Customer Convenience," Proc. the Canmaker Summit [CD-ROM], Singapore.

[3] Han, J., Yamazaki, K., and Nishiyama, S, 2004, "Optimization of the Crushing Characteristics of Triangulated Aluminum Beverage Cans," Structural and Multidisciplinary Optimization, **28**(1), pp. 47-54.

[4] Han, J., Itoh, R., Nishiyama, S., and Yamazaki, K., 2005, "Application of Structure Optimization Technique to Aluminum Beverage Bottle Design," Structural and Multidisciplinary Optimization, **29**(4), pp.304-311.

[5] Yamazaki, K., Itoh, R., Watanabe, M., Han, J. and Nishiyama, S., 2007, "Applications of structural optimization techniques in light weighting of aluminum beverage can ends," Journal of Food Engineering, **81**, pp.341–346.

[6] Yoshida, M., and Yoshizawa, T., 1996, Mitsubishi Materials Corporation, Tokyo, Japan Utility Model Application for a "Can end," Docket No. 2508637, filed 1996.

[7] Mounteastle, V. B., 1980, "Medical physiology," 14th ed., The CV Mosby Co, St Louis, Chap.11.

[8] Johamson, R.S. and Vallbo, A.B., 1983, "Tactile sensory coding in the glabrous skin of the human hand," Trends Neurosci, **6**, pp.27-32.

[9] Johansson, R.S. and Vallbo, A.B., 1979, "Tactile Sensibility in the Human Hand: Relative and Absolute Densities of Four Types of Mechanoreceptive Units in Glabrous Skin," The Journal of Physiology, **286**, pp.283-300.

[10] Goodwin, A.W. and Wheat, H.E., 1992, "Magnitude Estimation of Contact Force When Objects with Different Shapes are Applied Passively to the Fingerpad," Somatosensory and Motor Research. **9**(4), pp.339-344.

[11] Fransson-Hall, C. and Kilbom, A., 1993, "Sensitivity of the Hand to Surface Pressure," Applied Ergonomics, **24**, pp.181-189.
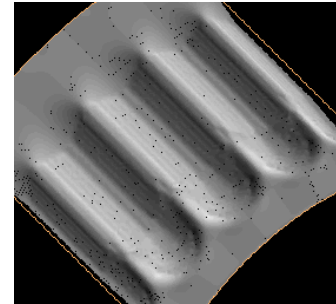
[12] Johansson, L., Kjellberg, A., Kilbom, A., and Hagg, G., 1999, "Perception of surface pressure applied to the hand," Ergonomics, **42**(10), pp.1274-1282.

[13] Brennum, J., Kjeldsen, M., Jensen, K. and Jensen, S.T., 1989, "Measurements of human pressure-pain threshold on fingers and toes," Pain, **38**, pp.211-217.

[14] Suzuki, K. and Nishihara, T., 2004, "The Design of Surface Shape of Resin Considering Tactile Sensation," Proc. 3rd China-Japan-Korea Joint Symposium on Optimization of Structural and Mechanical Systems, Kanazawa, Japan, pp.329-334.

[15] Horvath, I. And Zhang, B., 2005, "Status of Digital Human Body Modeling from the Aspect of Information Inclusion," Proc.of ASME IDETC/CIE 2005, DETC2005-84540.

[16] Srinivasan, M., Gulati J. and Dandekar, K., 1992, "In Vivo Compressibility of the Human Fingertip," Trans. of ASME, Advances in Biomechanical Engineering, **22**, pp.573-576.

[17] Srinivasan, M. and Dandekar, K., 1996, "An Investigation of the Mechanics of Tactile Sense Using Two-Dimensional Models of the Primate Fingertip," Trans. of ASME, Journal of Biomechanical Engineering, **118**, pp.48-55.

[18] Serina, E., Mockensturm, E., Mote Jr. D. and Rempel, D., 1998, "A Structural Model of the Forced Compression of the Fingertip Pulp," Journal of Biomechanics, **31**, pp.639-646.

[19] Serina, E., Mote Jr.D. and Rempel, D., 1997, "Force Response of the Fingertip Pulp to Repeated Compression – Effects of Loading Rate, Loading Angle and Anthropometry," Journal of Biomechanics, **30**(10), pp.1035-1040.

[20] Netter, H. F., 2004, "Atlas of Human Anatomy," Third Edition, Japanese Version, Nankodo, pp.454.

[21] Rho J.Y., Ashman R.B. and Turner C.H., 1993, "Young's Modulus of Trabecular and Cortical Bone Material: Ultrasonic and Microtensile Measurements," Journal of Biomechanics, **26**(2), pp.111-119.

[22] Aluminum Can Division, Stay-on-Tab pamphlet, Reynolds Metals Company, 1984.

[23] Han, J., Yamazaki, K., Itoh, R. and Nishiyama, S., 2006, "Multi-Objective Optimization of a Two-Piece Aluminum Beverage Bottle Considering Tactile Sensation of Heat and Embossing Formability," Structural and Multidisciplinary Optimization, **32**(2), pp.141-151.